

Original

Craus, M.L.; Anitas, E.; Cornei, N.; Islamov, A.; Haramus, V.M.:
**Magnetic Structure of La_{0.54}Ho_{0.11}Sr_{0.35}Mn_{1-x}Cu_xO₃
Manganites**
Solid State Phenomena, Magnetism and Magnetic Materials V (2012)
Trans Tech Publications

DOI: [10.4028/www.scientific.net/SSP.190.121](https://doi.org/10.4028/www.scientific.net/SSP.190.121)

Magnetic Structure of $\text{La}_{0.54}\text{Ho}_{0.11}\text{Sr}_{0.35}\text{Mn}_{1-x}\text{Cu}_x\text{O}_3$ Manganites

M.-L. Craus^{1,2,a,*}, E. Anitas^{2,3,b}, N. Cornei^{4,c}, A. Islamov^{2,d} and V. Garamus^{5,e}

¹ National Institute of Research and Development for Technical Physics, Mangeron 47, Iasi, Romania

² Joint Institute for Nuclear Research, Joliot-Curie 6, Dubna, Russia

³ Horia Hulubei National Institute of Physics and Nuclear Engineering, Atomistilor 407, Bucharest - Magurele, Romania;

⁴"Al. I. Cuza" University, Chemistry Department, Blvd. Carol I 11, Iasi, Romania

⁵ Institute of Materials Research, Geesthacht, Germany

^acraus@phys-iasi.ro, ^beanitasro@yahoo.com, ^cncornei@uaic.ro, ^dakhmed.islamov@gmail.com, ^evasyl.haramus@hzg.de, *corresponding author

Keywords: manganites, crystal/magnetic structure, transport properties, small-angle neutron scattering

Abstract. New $\text{La}_{0.54}\text{Ho}_{0.11}\text{Sr}_{0.35}\text{Mn}_{1-x}\text{Cu}_x\text{O}_3$ manganites were obtained by sol-gel method using oxides and acetates and sintered finally in air at 12000 C for 15 h. The samples were studied by X-ray diffraction, magnetic and electric methods. Space group, lattice constants, average size of the crystalline blocks and positions of cations/anions in the unit cell, were determined using the FullProf code. The samples contain only a perovskite phase with an orthorhombic structure (Pnma space group). Small-angle neutron scattering (SANS) measurements were performed on the SANS-1 setup at the FRG-1 reactor of the GKSS Research Centre (Geesthacht, Germany). The sizes of magnetic clusters have been determined at room temperature.

1. Introduction

The colossal magnetoresistance (CMR), which was observed in perovskite manganites, involves, besides the double exchange mechanism, electron-phonon interactions. Local distortions of the BO_6 octahedra in ABO_3 perovskite manganites determine the charge transport behavior and complex magnetic and crystal structures. Zener–de Gennes [1, 2] mechanism for double exchange offers a clear indication of a convenient way to control the coupling between the mobile holes and the localized t_{2g}^3 electrons. The band width depends on the bond angle ($\angle\text{Mn-O-Mn}$) and on the Mn-O distance ($d_{\text{Mn-O}}$) of the Mn–O–Mn bonds. More attention was paid to the compounds corresponding to $x \approx 0.3$, where the magnetoresistance attains its maximum value. The interactions of the local Jahn–Teller distortions with the charge carriers determine the transport behavior above the Curie temperature [3]. The partial substitution of La with Ho in $\text{La}_{0.7-x}\text{Ho}_x\text{Sr}_{0.3}\text{MnO}_3$ leads to a decrease of the unit cell volume and of the Curie temperature [5], due to an increase of the distortion of the lattice, a weakening of the double exchange (DE) interaction and a corresponding decrease of the Curie temperature of $\text{La}_{0.7-x}\text{Ho}_x\text{Sr}_{0.3}\text{MnO}_3$ manganites [4]. Concerning the effect of Cu on magnetic properties, Dubroka et al. [5] showed that the Curie temperature of $\text{La}_{1-x}\text{Sr}_x\text{Mn}_{1-y}\text{Cu}_y\text{O}_3$ decreases with the increase of Cu concentration, if the ratio of Mn^{4+} and Mn^{3+} concentrations remains about 0.32. The aim of present paper is to investigate the correlation between the Cu content, crystal structure, magnetic structure and transport characteristics in $\text{La}_{0.54}\text{Ho}_{0.11}\text{Sr}_{0.35}\text{Mn}_{1-x}\text{Cu}_x\text{O}_{3-\delta}$ (LHSMCO) manganites.

2. Experimental

The samples with the chemical composition $\text{La}_{0.54}\text{Ho}_{0.11}\text{Sr}_{0.35}\text{Mn}_{1-x}\text{Cu}_x\text{O}_{3-\delta}$ were prepared by means of the sol-gel method, using as precursors rare-earth oxides (La_2O_3 and Ho_2O_3) (purity: 99.99%), Sr and Mn acetates, and Cu nitrate (purity: 99.00%) [6]. Details of the XRD, magnetic and electrical

measurements will be presented elsewhere. The small-angle neutron scattering (SANS) measurements were carried out on the SANS-1 setup in the absence of applied magnetic field at the FRG-1 reactor of the GKSS Research Centre (Geesthacht, Germany).

3. Results and Discussions

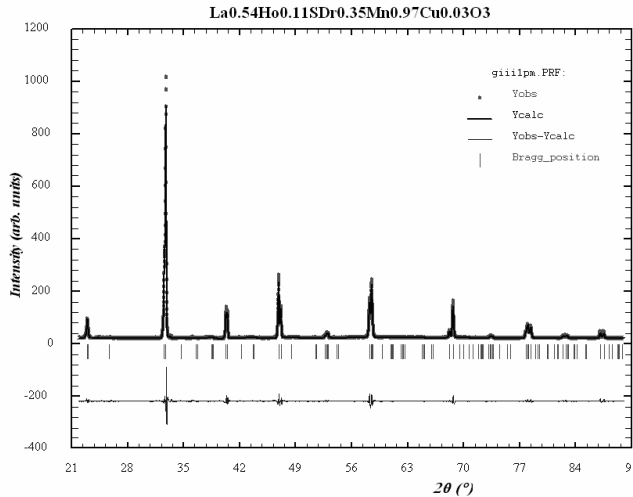


Figure 1. Observed (Y_{obs}) and calculated (Y_{calc}) X-ray diffraction patterns, difference between them ($Y_{\text{obs}}-Y_{\text{calc}}$), and the Bragg positions for $\text{La}_{0.54}\text{Ho}_{0.11}\text{Sr}_{0.35}\text{Mn}_{0.97}\text{Cu}_{0.03}\text{O}_3$ manganite (FullProf method)

Table 1). The observed B-O distance, and hence the ionic radius at B sites, decrease slowly with increasing Cu content in the samples (see Table 1).

Table 1. Dependence on Cu content (x) of the lattice constants (a , b , c), unit cell volume (V), average size of crystalline blocks (D_{cb}), microstrains (ε), observed average distances between B and O sites ($\langle d_{\text{BO}} \rangle_{\text{obs}}$), bandwidth (w) and observed tolerance factor (t_{obs}) in $\text{La}_{0.54}\text{Ho}_{0.11}\text{Sr}_{0.35}\text{Mn}_{1-x}\text{Cu}_x\text{O}_3$ manganites

x	a [Å]	b [Å]	c [Å]	V [Å ³]	D_{cb} [Å]	ε	$\langle d_{\text{BO}} \rangle_{\text{obs}}$ [Å]	$\langle \angle \theta_{\text{BOB}} \rangle$ [°]	w	t_{obs}
0.03	5.4650	7.7096	5.4982	231.655	816	0.00049	1.9424	170.39	0.098	0.9280
0.06	5.4647	7.7090	5.4990	231.658	781	0.00016	1.9332	172.17	0.099	0.9277
0.15	5.4644	7.7089	5.4995	231.662	748	0.00031	1.9239	171.34	0.101	0.9314

From XRD data concerning the positions of cations and anions in the unit cell, we obtained the average B-O distances and the observed tolerance factors ($\langle d_{\text{BO}} \rangle_{\text{obs}}$, t_{obs} , see Table 1). The variation of the unit cell volume could be explained by the decrease of average ionic radii at B sites with the increase of Cu content (if oxygen concentration remains unchanged) and the increase of r_{B} with the increase of oxygen concentration (for the same concentration of cations in all samples). The bandwidth ($w \propto \cos\{\frac{\pi - \angle \text{BOB}}{2}\} / (d_{\text{BO}})^{3.5}$) increases with decreasing d_{BO} , despite the existence of a peak in the observed dependence of the B-O-B bond angle on the Cu content (see Table 1). The SANS results concerning manganites with the concentrations of Cu equal to 0.03, 0.06, and 0.15 clearly demonstrate two different levels (see Fig. 2). In the first level ($0.005 \text{ \AA}^{-1} < q < 0.015 \text{ \AA}^{-1}$) the scattering intensity $I(q)$ follows classical Porod law ($I(q) \sim q^{-4}$), and corresponds to the nuclear scattering by particles with smooth surfaces (see Fig. 2). The power law with the exponent $\alpha < 3$ is typical for small-angle scattering from mass fractals structures (see Fig. 2 and Table 2) and, in this case, α characterizes the mass fractal dimension of the system.

The sintered samples contain only one phase, with orthorhombic structure ($Pnma$ space group) (see Fig. 1), in agreement with the available data [7]. The micrographs of the manganites indicated also the presence of only one phase and a significant increase of the average size of the crystallites with the increase of the Cu content in the samples (results will be published). It is known that the manganite structure is formed by chains of MnO_6 octahedra. For magnetic and transport properties the oxygen position and, hence Mn-O distances and Mn-O-Mn bond angles play an important role.

The unit cell volume and lattice constant c slowly increase, while a and b lattice constants decrease with increasing Cu concentration (x) (see Table 1). The average size of crystalline blocks (D_{cb}) decreases with x , while the microstrains have a minimum at $x = 0.06$ (see

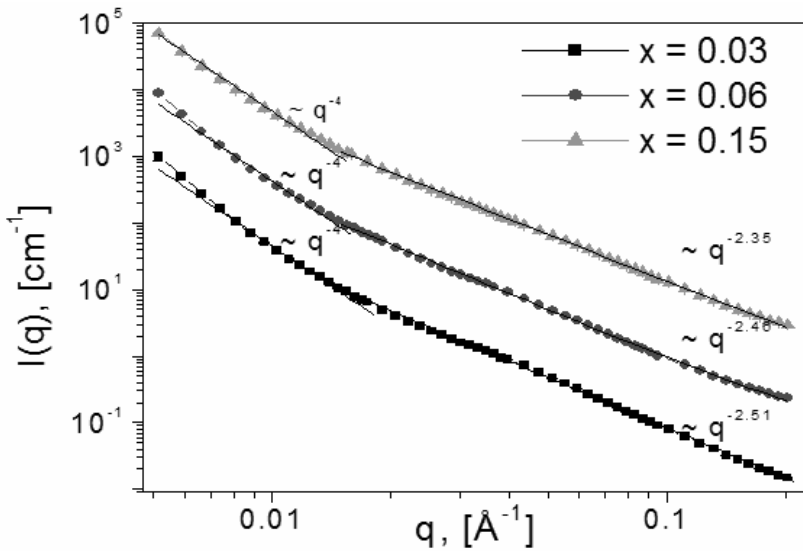


Fig. 2. Small-angle neutron scattering intensities for $\text{La}_{0.54}\text{Ho}_{0.11}\text{Sr}_{0.35}\text{Mn}_{1-x}\text{Cu}_x\text{O}_3$ manganites at different Cu concentrations and the corresponding power-law fits. ($I(q)$ values were multiplied by 10 for $x = 0.06$ and by 100 for $x = 0.15$).

The higher is the value of α the more compact is the structure (e.g. in the case of highly branched clusters). The fractal dimension decreases with increasing Cu content. It is an indication a looser structure at higher values of Cu content. Since the crystallites have sizes D of about $2 \mu\text{m}$, the nuclear scattering decreases quickly for $q > 2\pi/D$. Therefore, the second level of scattering corresponds to the scattering by magnetic polydispersed clusters. In the absence of the applied magnetic field, both the nuclear and magnetic scattering are isotropic over the radial angle

and the total neutron scattering intensity is given by $I(q) = I_{\text{nuc}}(q) + I_{\text{mag}}(q)$. After subtraction of nuclear scattering from total scattering intensity, we obtain the magnetic scattering. The program GNOM [8] was used for calculations of the pair distance distribution function (PDDF) and the radius of gyration R_g of magnetic clusters (see Fig. 3 and Table. 2).

Table 2. Variation of the gyration radius (R_g), calculated maximum size (D_{max}), calculated volume of magnetic clusters (V_{in}), and fractal dimension (α) with Cu concentration (x)

x	$R_g[\text{\AA}]$	$D_{\text{max}}[\text{\AA}]$	$V_{\text{in}}[\text{\AA}^3]$	α
0.03	43.9 ± 0.9	136.5	217800	2.51
0.06	51.5 ± 0.5	160.0	249500	2.46
0.15	54.4 ± 0.5	170.0	280100	2.35

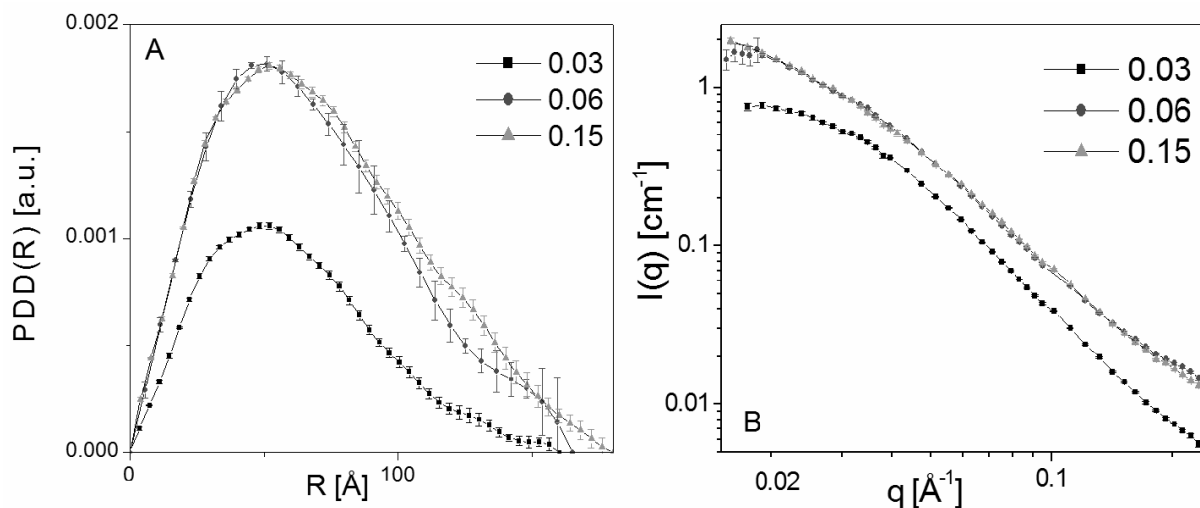


Fig. 3. Magnetic scattering from $\text{La}_{0.54}\text{Ho}_{0.11}\text{Sr}_{0.35}\text{Mn}_{1-x}\text{Cu}_x\text{O}_3$ manganites (A) and their pair distance distribution functions (B) at Cu concentrations: $x = 0.03(\blacksquare)$, $0.06(\blacktriangle)$, and $0.15(\blacktriangledown)$.

The atomic simulation performed by Tang et al. [9] confirmed the experimental results concerning the structural inhomogeneities [10] and a tendency to the formation of magnetic clusters, about 1 nm in diameter, around Sr cations [9]. We have performed the calculations with DAMMIN program [11] and determined average values of the maximum size (D_{max}) of magnetic clusters, their volume

(V_{in}) and shape. With the growth of Cu content, we observed an increase of R_g , D_{max} , and V_{in} (see Table 2). The magnetic clusters have an elongated irregular shape and diameters of about 15 nm. They are about six times smaller than the average size of coherent blocks (see Tables 1 and 2). The results concerning magnetoresistance and magnetic properties will be published soon.

4. Conclusions

We obtained a series of $La_{0.54}Ho_{0.11}Sr_{0.35}Mn_{1-x}Cu_xO_3$ manganites, with the orthorhombic structure. The crystal structure undergoes only a slight change in the investigated range of compositions. Small Cu concentration in the $La_{0.54}Ho_{0.11}Sr_{0.35}Mn_{1-x}Cu_xO_3$ manganites produces a pronounced effect on the magnetoresistance near room temperature. This behavior can be attributed to the nanomagnetic clusters existing in the sample even in the vicinity of room temperature. The average size of magnetic domains increases with the Cu content in the samples.

The SANS measurements ($H = 0$, room temperature) suggest the existence of an appreciable concentration of magnetic phase near Curie temperature due to metallic magnetic clusters. At room temperature, the total concentration of these clusters seems to have a minimum for the sample with $x = 0.06$, in agreement with the data obtained from the temperature dependence of resistivity and molar magnetization.

References

- [1] C. Zener, Phys. Rev. 82 (1951) 403.
- [2] P.-G. De Gennes, Phys. Rev. 118 (1960) 141.
- [3] N.D. Mathur, P.B. Littlewood, Solid State Commun. 119 (2001) 271.
- [4] P. Raychaudhury, T.K. Nath, P. Sinha, C. Mitra, A.K. Nigam, S.K. Dhar, R. Pinto, J. Phys.: Condens. Matter 9 (1997) 10919.
- [5] A. Dubroka, J. Humlíček, M.V. Abrashev, Phys. Rev. B 73 (2006) 224401.
- [6] M.-L. Craus, N. Cornei, I. Berdan, C. Mita, M.N. Palamaru, Ceramics Intern. 30 (2004) 447.
- [7] S. Asthana, A.K. Nigam, D. Bahadur, Phys. Stat. Solidi (b) 243 (2006) 1922.
- [8] D.I. Svergun, J. Appl. Cryst. 24 (1991) 485.
- [9] F.L. Tang, X. Zhang, Y. Shao, J. Phys.: Condens. Matter 18 (2006) 5579.
- [10] T. Shibata, B. Bunker, J. F. Mitchell, P. Schiffer, Phys. Rev. Lett. 88 (2002) 207205.
- [11] D. I. Svergun, Biophys. J. 76 (1999) 2879.